

0453

REPORT DOCUMENTATION PAGE

OMB NO. 0704-0188

Public reporting burden for this collection of information is estimated to average 1 hour per response, including the time for reviewing instructions, searching existing data sources, gathering and maintaining the data needed, and completing and reviewing this collection of information. Send comments regarding this burden estimate or any other aspect of this collection of information, including suggestions for reducing this burden, to Washington Headquarters Services, Directorate for Information Operations and Reports (0704-0188), 1215 Jefferson Davis Highway, Suite 1204, Arlington, VA 22202-4302. Persons should be aware that notwithstanding any other provision of law, no person shall be subject to any penalty for failing to comply with a collection of information if it does not display a currently valid OMB number. PLEASE DO NOT RETURN YOUR FORM TO THE ABOVE ADDRESS.

1. REPORT DATE (DD-MM-YYYY) 12-12-2002		2. REPORT TYPE Final Performance		3. DATES COVERED (From - To) 01-APR 2001 to 31 MAR	
4. TITLE AND SUBTITLE Phase Stability in Ultra-High Temperature Refractory Metal Alloys Alloys and Coatings				5a. CONTRACT NUMBER	
				5b. GRANT NUMBER F49620-01-1-0296	
				5c. PROGRAM ELEMENT NUMBER	
6. AUTHOR(S) Professor John H. Perepezko				5d. PROJECT NUMBER	
				5e. TASK NUMBER	
				5f. WORK UNIT NUMBER	
7. PERFORMING ORGANIZATION NAME(S) AND ADDRESS(ES) University of Wisconsin-Madison Research Administration 750 University Ave. Madison, WI 53706				8. PERFORMING ORGANIZATION REPORT	
9. SPONSORING / MONITORING AGENCY NAME(S) AND ADDRESS(ES) AF Office of Scientific Research Research/NA (Dr. C. Hartley) 801 N. Randolph Street Arlington, VA 22203				10. SPONSOR/MONITOR'S ACRONYM(S)	
				11. SPONSOR/MONITOR'S REPORT NUMBER(S)	
12. DISTRIBUTION / AVAILABILITY STATEMENT Approved for public release; distribution unlimited.					
13. SUPPLEMENTARY NOTES					
14. ABSTRACT The experimental determination of phase stability in very high temperature refractory metal (RM) base alloys such as those in the Mo-Si-B system and the evaluation of thermal barrier and oxidation resistant coatings for these systems requires very high temperature annealing furnaces with long term capability to 2400 °C under vacuum and inert atmosphere conditions. Moreover, in order to establish quantitative phase stability data for key phase reactions and to evaluate fully the kinetics of coating reactions, the acquisition of a very high temperature DTA/TGA system represents a critical experimental capability. With an effective phase stability model, data from measurements at a few temperatures may be extrapolated over a wide range of temperature and the influence of additional alloying components may be assessed effectively in order to enable the computational design of optimal alloy and coating constitution for high temperature performance. The combination of a very high temperature annealing facility and a high temperature DTA/TGA system represents a powerful and very effective enhancement of the experimental capabilities that are necessary in order to complete the current studies and provides an essential base for continued evaluation of very high temperature materials systems for structural applications. Both components of the high temperature analysis facility have been purchased under the grant. The facilities are being installed and tested and will be utilized also in educational developments for class projects and for the training of undergraduate and graduate students in the evaluation of ultrahigh temperature phase stability and coating reactions in structural materials.					
15. SUBJECT TERMS High Temperature Alloys, Refractory Metals, Phase Stability, Thermal Analysis,					
16. SECURITY CLASSIFICATION OF:			17. LIMITATION OF ABSTRACT	18. NUMBER OF PAGES 19	19a. NAME OF RESPONSIBLE PERSON
a. REPORT	b. ABSTRACT	c. THIS PAGE			19b. TELEPHONE NUMBER (include area code)

Standard Form 298 (Rev. 8-98)
Prescribed by ANSI Std. Z39.18

20030210 143

TABLE OF CONTENTS

Abstract

Budget

Summary of facility acquisition expenditure

Supporting Information

- 3. 1. Introduction
- 3. 2. Phase Stability in the Mo-rich Mo-Si-B System at 1600°C
- 3. 3 Solidification Pathways of Mo-rich Portion of the Mo-B-Si System
- 3. 4 Single Phase T₂
- 3. 5 Growth Kinetics Involving the T₂ Phase Formation
- 3. 6 Refractory Metal Substitution for Mo in the Mo-Rich Mo-B-Si Alloys
- 3. 7 New Research Opportunities
- 3. 8 Research Related Education

References

Acquired Equipment Facilities

The grant budget covered the cost for the acquisition of an ultra high temperature furnace for temperature range of 25 - 2500°C and a simultaneous DTA/TGA for thermal analysis in the temperature range of 25 - 2000°C . The detailed description of the facilities and the acquisition costs is provided in the following discussion.

ULTRA-HIGH TEMPERATURE FURNACE SYSTEM

- **Model # T-3X6-WM-2500-V/G**
- **Manufactured by Materials Research Furnaces, Inc.**
Suncook Business Park, Route 28, Suncook New Hampshire 03275
- **Contact person: Daniel J. Leary.**
Phone # (603) 485-2394 Fax # (603) 485-2395 E-mail: mrf@interserv.com

➤ **Equipment Capabilities:**

1. Hot Zone

Normal operating temperature is 2500°C. It has 3 " diameter and 6 " high hot zone, sufficient large space for DC as well as annealing treatment specimens. The heating element is made of Tungsten mesh with Tungsten/Molybdenum sheet heat shield. The specimens are supported on a Tungsten hearth plate.

2. Temperature Control

Eurotherm 3000 series Digital controller is used with a type C thermocouple, sheathed with a Two Color Optical Pyrometer. For over-temperature controller, the Eurotherm 93 digital controller is used equipped with a type C thermocouple.

3. Furnace Chamber

Top access, water cooled, round, double wall 304L stainless steel Vacuum Chamber with a #4 polish on the inside and electropolished. Top cover and bottom covers are Nickel Plated Copper, water cooled. Both top and bottom covers are protected with copper cooling plates. A rotatable quartz sight window w/ inert gas protection is provided.

4. Power to the heating elements is supplied by 1 phase SCR controlled (35Kva) with modulating ramp rate, water cooled power cables and Volts and amp meters.

5. Installation: Require 40 Kva power source with 208/240/480 voltage 1 phase/60 Hertz.

Cooling system requires 7-8 GPM water flow at 50 PSIG and 70°F

Gas system needs 30 LPM at 50 PSIG.

6. Warranty: 1 year warranty for all components except for consumable items

7. Estimated Lifetime: 7 years

- *Quoted price for base unit with furnace chamber, hot zone, inert gas system, 40 Kva power supply, basic controls, water manifold, furnace mount, ISO 100 turbo pumping system, two-color optical pyrometer and automatic thermocouple remover (ATR) and type "C" thermocouples with installation at UW-Madison*

SUB-TOTAL \$104,725.00

Manufacturer Recommended Cooling System (Scheiber Eng. # 1001AC
water chilled closed loop system using H₂O and dual refrigeration)

\$17,270.00

TOTAL COST FOR MANUFACTURER RECOMMENDED BASE UNIT \$121,995.00

- *Quoted price for the cost of the consumable items*
- Heating element Tungsten Mesh 3 " Dia. X 6 " long \$ 3,450.00
- Set of Tungsten & Molybdenum Heat Shield 4W/2M \$ 5, 895.00
- SUB-TOTAL \$9,345.00

TOTAL COST FOR ULTRA-HIGH TEMPERATURE FURNACE SYSTEM \$ 131,340.00

SIMULTANEOUS ULTRA-HIGH DTA-TGA

- **Model # STA 409 C/7/F**
- **Manufactured by Netsch Instruments, Inc., P. O. Box 4469 Estes Park, CO 80517 USA**
- **Contact Person: Dr. Jack Henderson**
Phone: 970-577-0840 Fax: 970-577-1224 E-mail: j_bhenderson@email.msn.com
- **Equipment Capabilities**
- A. **Measuring parts**
 - Weighing system with electromagnetic compensation range 500 mg, with mechanic tare switch system, range 15 g, switch-able in 100 mg steps and continuously, integrated preamplifies for dT and TG
 - High temperature furnace with bifilar slotted graphite heating element, fiber insulation and inner protective tube of graphite, furnace shell of stainless steel, vacuum tight and water cooled, control thermocouple W3%Re-W25%Re, temperature range 25 – 2000C, max. temp. 2000°C, max. power consumption 5,0 kW, operation under protective gas atmosphere (helium , argon).
 - Sample carries system for simultaneous TG-DTA measurements, complete with radiation shield and thermocouple W3%Re-W25%Re.
 - Refrigerated bath circulator, heating capacity 1000W, cooling capacity 350 W (at 20°C), temperature stability of 0.03 K, complete with 10 m tubing and connection parts.
- B. **Control, Measurements and Data Acquisition**
 - Plug in power unit, SCR controlled, with control amplifier, current limit feedback, adjustable between 50 and 100% of the output current.
 - Output insulating transformer 5 kVA, 230/25, 30, 35 V
 - Safety control system for the operation of the highest temperature furnaces with function switches, flow control and displays for protective gas operation and cooling water.
 - TA system controller TASC 414/3 for data acquisition and temperature control.
 - Evacuating system for furnace and sample chamber
- C. **Software and Computer System**
 - Computer system: Desktop-PC, Pentium III 600MHz, RAM 64 MB, HD 8.4 GB, CD-ROM 32X, Disk 3.5"/1.44 MB, Monitor 17" Ultra VGA, Window 95/NT 4,0 , interfaces: serial, parallel, USB.
 - Software package for STA 409 for data acquisition, storage and evaluation with the following capabilities:
 - Choice of versatile possibilities of temp. control (max 96 program steps)

- Graphic presentation of the measuring data during the test in absolute or relative units such as DSC/mV or heat flux/mW, TG/mg or TG/%.
- Semi-automatic routines for the determination of characteristic temperatures (extrapolated onset peak maximum, peak end) and for DSC glass transition (Tg-On, Tg-Mid, Tg-End, Tg-Infl, delta cp).
- Fully automatic routine for complex peak evaluation (onset, points of inflection, peak, end point, peak height, peak width, peak area).
- Determination of DSC peak areas and partial areas using 5 base lines (linear, area-proportional).
- Semi-automatic routine for the evaluation of mass change (temperature/time and step size) on single steps or fully automatically on the total curve, determination of the remaining mass.
- Graphic export as HPGI files or into the WINDOWS clipboard for use in word processing program
- Inkjet printer DeskJet 895 Cxi with connection cable
- Estimated Lifetime: 7 years

- **Quoted price for the simultaneous DTA-TGA equipment:** \$ 125, 000.00
- **Quoted price for the Tungsten sample crucibles** \$ 3,000.00

TOTAL \$128,000.00

SUMMARY OF FACILITY ACQUISITION EXPENDITURE

A.	Ultra-High Temperature Furnace	
	➤ Base unit with installation	\$104,725.00
	➤ Manufacturer Recommended Cooling System	\$17,270.00
	MANUFACTURER RECOMMENDED BASE UNIT	\$121,995.00
	➤ Cost of the consumable items	\$9,345.00
	TOTAL COST FOR ULTRA-HIGH TEMPERATURE FURNACE SYSTEM	\$ 131,340.00
B.	Simultaneous Ultra-High DTA-TGA System	
	➤ DTA-TGA equipment	\$125,00.00
	➤ Cost of the consumable item	\$ 3,000.00
	TOTAL COST FOR ULTRA-HIGH DTA-TGA SYSTEM	\$ 128,000.00
	TOTAL REQUESTED BUDGET FOR THE ULTRA HIGH TEMPERATURE FACILITY	\$ 259,340.00

3. Research summary

3.1 Introduction

High temperature structural materials play a pivotal role as critical components in a number of key defense technologies as well as energy production, transportation and advanced aerospace propulsion systems. The challenging performance demands of structural integrity and environmental resistance at elevated temperature have traditionally required Ni-base superalloys. However, superalloys have been optimized so that further increase in service temperature is not probable. A new class of metallic materials based upon refractory metal(RM)-B-Si alloys has been identified in current programs under AFOSR sponsorship as qualified for use above 1500°C. The current studies of phase stability and coating reactions have made good progress in establishing a fundamental understanding of the alloy behavior below about 1600°C, but the systems of interest have a higher temperature capability and in fact estimates from the current work indicate melting above 2000°C. At the same time the progress in the current work has been hampered by sluggish diffusional reactions at the limit of our current capability (1600°C). A higher annealing temperature capability is required to allow for a complete study of phase stability. Based upon the findings in the current work, it is also apparent that a high temperature DTA/TGA (Differential Thermal Analysis/ ThermoGravimetric Analysis) would add new capability for quantitative measurements of key phase transition temperatures, critical thermodynamic data and permit a full analysis of coating reaction kinetics. The following sections present the justification for the high temperature facility to enhance the current capability and the identification of new directions of research that have been enabled by the acquired equipment as well as the impact on research related education.

3.2 Phase Stability in the Mo-rich Mo-Si-B System at 1600°C

Based upon the EPMA examination of phase compositions of the long-term annealed as-cast samples and rapidly solidified samples and x-ray diffraction determination of phase identity, the isothermal section for the Mo-Si-B system at 1600°C has been constructed as shown in Figure 1. Since the boundary lines are plotted on the basis of composition data of homogeneous phases obtained using EPMA, the boundaries are drawn as a broken line. Moreover, the present study concentrates on the Mo-MoB-Mo₅Si₃ region excluding the two-phase equilibrium region of MoB-Mo₅Si₃. Accordingly the ternary isothermal section in Figure 1 does not contain a complete boundary of MoB-Mo₅Si₃ two-phase equilibrium region. This gives incomplete compositional boundaries of both the B-rich side of MoB and the Si-rich side of Mo₅Si₃. The compositional homogeneity region of Mo₂B ranges from ~33 at%B to ~39 at%B and has Si solubility range to ~1 at%Si. The B-rich boundary composition of Mo₂B yields the possibility of existence of Mo₃B₂ that is metastable at temperatures from 1900°C to 2080°C [92Asm]. However, x-ray diffraction determination of phase identity by Nunes *et al.* [97Nun] verified that the Mo₂B phase is in equilibrium with MoB and Mo solid solution (Mo-ss) at 1600°C. The MoB phase has a compositional homogeneity region higher than ~47 at%B and Si solubility range to ~2 at%Si. The Mo-ss phase does have negligible B solubility, but appreciable Si solubility to ~3 at%Si. The Mo₃Si phase has compositional homogeneity region of 22-26 at%Si and negligible B

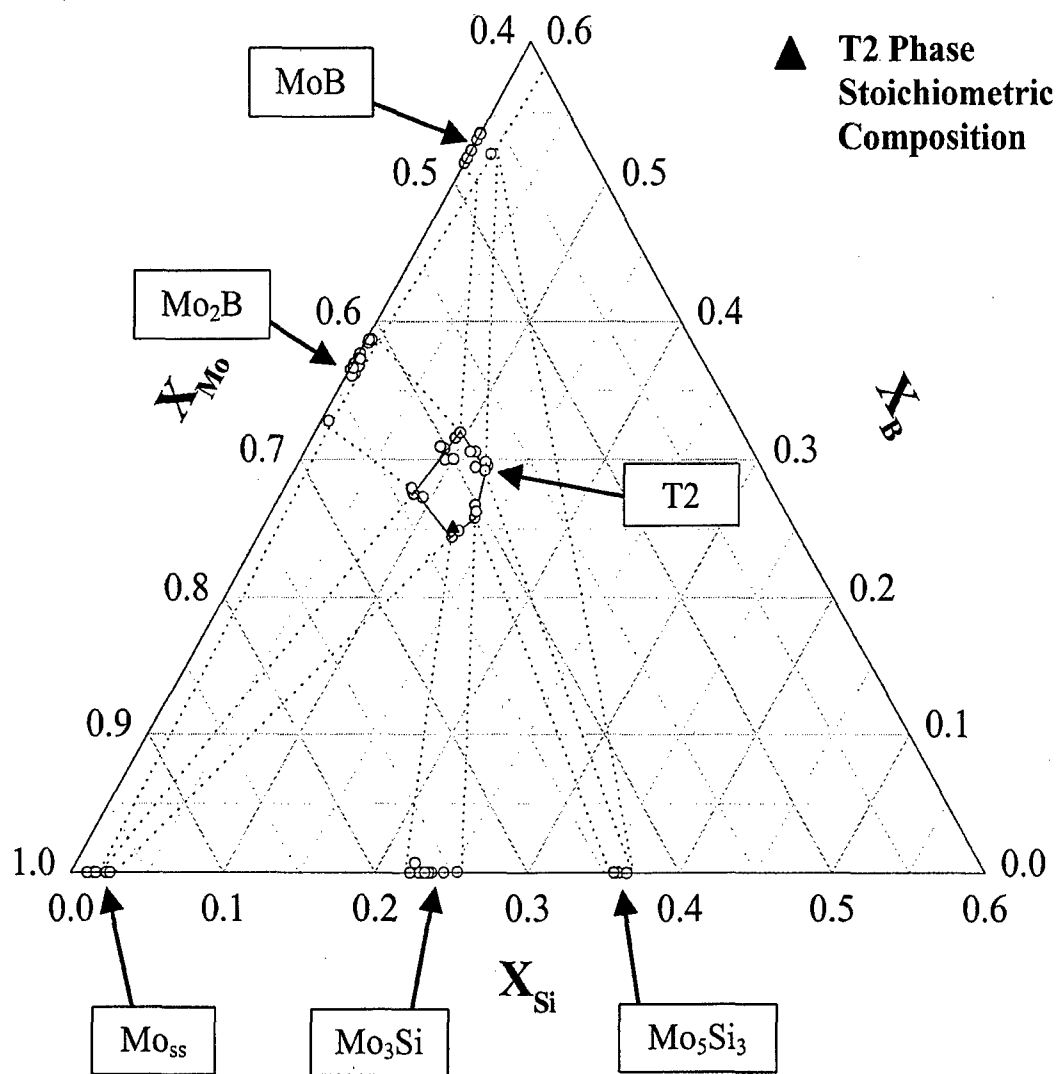


Figure 1 The ternary isothermal section of the Mo-rich Mo-Si-B system showing the phase boundaries.

solubility of <1 at%B. The compositional boundary of Mo_3Si_3 on the Mo-rich side extends to ~ 35 at%Si. The T_2 phase has a Si solubility range of 8-13.65 at%Si as well as a B solubility range of 23.3-32.35 at%B. The T_2 phase has an appreciable compositional homogeneity range around the stoichiometric composition.

The finding on the appreciable non-stoichiometric homogeneity range of the T_2 phase is also reflected in the variation in the lattice parameters of the T_2 phase. While in general the higher the ratio of B to Si content in the T_2 phase, the smaller the lattice dimension of the tetragonal crystal, there is also strong evidence which points to the presence of multiple types of defect mechanisms operating within the homogeneity range of the T_2 phase. This can not be associated simply to the presence of thermal defects. Investigation is currently underway to unravel the roles of these multiple defect mechanisms and will be integrated to the thermodynamic modeling of the T_2 phase.

Critical to this issue is the ability to observe a larger homogeneity range in the T_2 phase since a larger phase field allows for a clearer delineation of the influence of the defect mechanism on the stability of the T_2 phase. To achieve this objective, a higher annealing temperature is required ($> 1600^\circ\text{C}$) and such a temperature range can not be achieved with the current annealing facility.

3.3 Solidification Pathways of Mo-rich Portion of the Mo-B-Si System

The solidification pathways of the Mo-rich portion in the Mo-B-Si system have been carefully assessed and the liquidus projection associated with the solidification sequences in the as-cast alloys has been thoroughly examined as shown in Figure 2. The most important finding is the extensive degree of segregation in the arc-cast alloy. This can be attributed to the extended liquidus region of some of the high melting borides such as Mo_2B and MoB phases. In general, the extended freezing range of the boride phases hinders the observation of some of the melting events for compositions that are of significant interest such as the stoichiometric T_2 phase compositions as well as the eutectic $\text{Mo}(\text{ss}) + T_2$ compositions. In fact, four types of solidification pathways involving different primary phases have been identified within the two-phase field region depending on the composition as schematically shown in Figure 3:

1. For Mo alloys with $0 < \text{B} < 14$ at. % and $0 < \text{Si} < 7$ at. %:
 $\text{Mo}(\text{ss})$ non-faceted dendritic primary $> \text{Mo}(\text{ss}) + \text{Mo}_2\text{B}$ eutectics $> \text{Mo}(\text{ss}) + T_2$ eutectics $> \text{Mo}_3\text{Si} + T_2$ co-precipitation.
2. For Mo alloys with $14 < \text{B} < 19$ at. % and $7 < \text{Si} < 8.5$ at. %:
 Mo_2B faceted columnar primary $> \text{Mo}(\text{ss}) + \text{Mo}_2\text{B}$ co-precipitation $> \text{Mo}(\text{ss}) + T_2$ eutectics $> \text{Mo}_3\text{Si} + T_2$ co-precipitation.
3. For Mo alloys with $19 < \text{B} < 22.5$ at. % and $8.5 < \text{Si} < 11.25$ at. %:
 T_2 faceted columnar primary $> \text{Mo}(\text{ss}) + T_2$ eutectics $> \text{Mo}_3\text{Si} + T_2$ co-precipitation
4. For Mo alloys with $19 < \text{B} < 22.5$ at. % and $8.5 < \text{Si} < 11.25$ at. %:

Although there is a transition in primary phase selection with changing composition across the $\text{Mo}(\text{ss}) + T_2$ two phase field, the final solidification reaction in the sequence, as a consequence of the segregation during solidification, is always the co-precipitation of $\text{Mo}_3\text{Si} + T_2$ as a eutectic with the Mo_3Si phase as the matrix. The formation of the Mo_3Si phase matrix further hinders the attainment of equilibrated $\text{Mo}(\text{ss}) + T_2$ two-phase microstructures due to the sluggish dissolution kinetics of the segregation induced phases. It is evident that extended

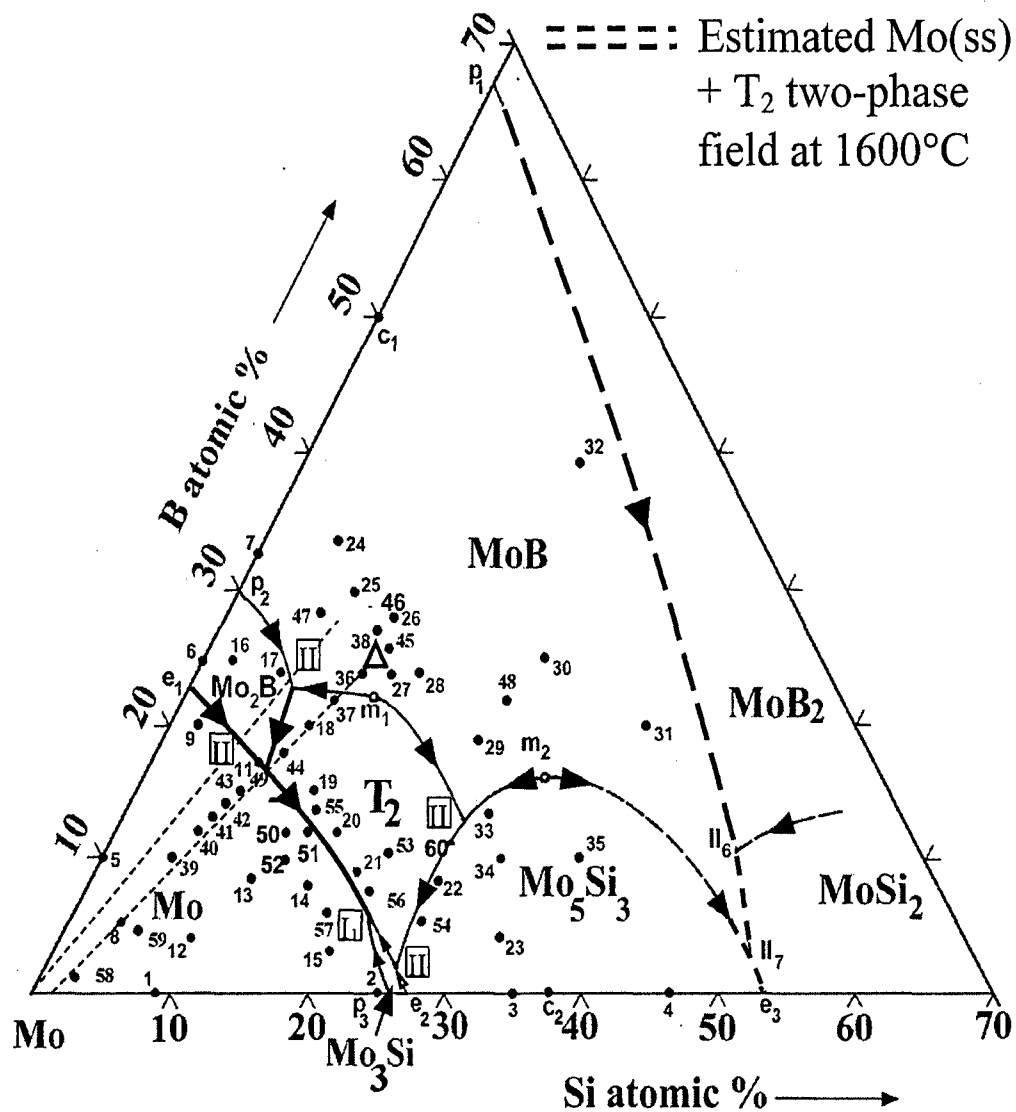


Figure 2: The liquidus projection on the Mo-rich portion of Mo-Si-B ternary system. The region bordered by the dotted lines represents the estimated location of Mo(ss) + T₂ two-phase field at 1600°C. The triangle point represents the stoichiometric T₂ phase composition.

annealing at 1200 °C yields almost no change in the as-cast microstructure. In fact, experience has also demonstrated that annealing at 1600 °C for 150 hours is not sufficient to dissolve the Mo_3Si and Mo_2B phases [97Per]. Even after this extended annealing treatment, the microstructures of the resulting alloys are not uniform as the remnants of the solidification morphology is clearly retained. The issue of solidification segregation is a major point in assessing the phase stability in the Mo-Si-B system. Furthermore, the non-homogeneous distribution of the two phases can not be readily modified by subsequent materials processing to obtain desired microstructures with optimal mechanical and physical properties. This experience clearly indicates that annealing treatments well above 1600°C are required to confirm the phase stability. However, our current capability does not allow for this capability. For long term annealing a very high temperature furnace with a capability to above 2400°C is necessary on a dedicated basis.

Based on our assessment on the solidification pathways in the arc-cast samples, the liquidus surface in general is quite shallow particularly in the vicinity of the two-phase field. This can be attributed to the high thermal stability of the Mo(ss) phase as well as the T_2 phase (the T_2 phase melts at about 2100-2200°C). This provides the opportunity to modify the solidification pathways so that the formation of boride phases can be essentially bypassed and thus the segregation can be significantly reduced. This will allow us to construct a more efficient annealing as well as thermo-mechanical treatment to yield the desired microstructure. need to elucidate the phase equilibria for temperatures above 1600°C.

3.4 Single-phase T_2

It is desirable to examine the possibility of producing the T_2 -phase directly from the melt. As noted in the Mo- T_2 plethral section (see Figure 3), the T_2 phase melts incongruently so that MoB would solidify first in as-cast alloys with a T_2 -stoichiometric composition ($\text{Mo}_{62.5}\text{B}_{25}\text{Si}_{12.5}$). The solidification path then proceeds with T_2 phase formation through a peritectic reaction of $\text{MoB} + \text{L} \rightarrow \text{T}_2$. The Mo_3Si and Mo_5Si_3 phases then form as the last parts to solidify. Hence, the production of the T_2 phase via conventional casting would be very challenging due to severe solidification segregation involving phases such as MoB and Mo_5Si_3 , which exhibit sluggish dissolution. In fact, arc-melted alloys with this composition still maintained the four phases in the microstructures even upon annealing at 1600°C for 150 hours. Thus, the formation of single-phase T_2 by conventional casting necessitates an extensive annealing procedure at very high temperatures i.e. in excess of 1600°C.

For these conditions, RSP can be very useful in suppressing the solidification segregation through the development of high melt undercooling and rapid interface velocities. Splat-quenched alloys with a T_2 stoichiometric composition, in contrast to the as-cast alloys, exhibited only a single T_2 phase. This was confirmed by the XRD measurements indicating only the T_2 phase in splat samples. The RSP products unfortunately are limited in size and therefore further consolidation processing is required. We are currently examining the powder processing routes with a number of varied powder constituents to promote an effective solid state synthesis of the T_2 phase in the bulk form. The current capability to sinter the powder is limited to the sluggish kinetics involved even with the powder mixture that utilizes the most effective diffusion pathways for the single phase T_2 synthesis. High temperature annealing treatment at ultra high temperature region beyond 1600°C is clearly necessary for this purpose.

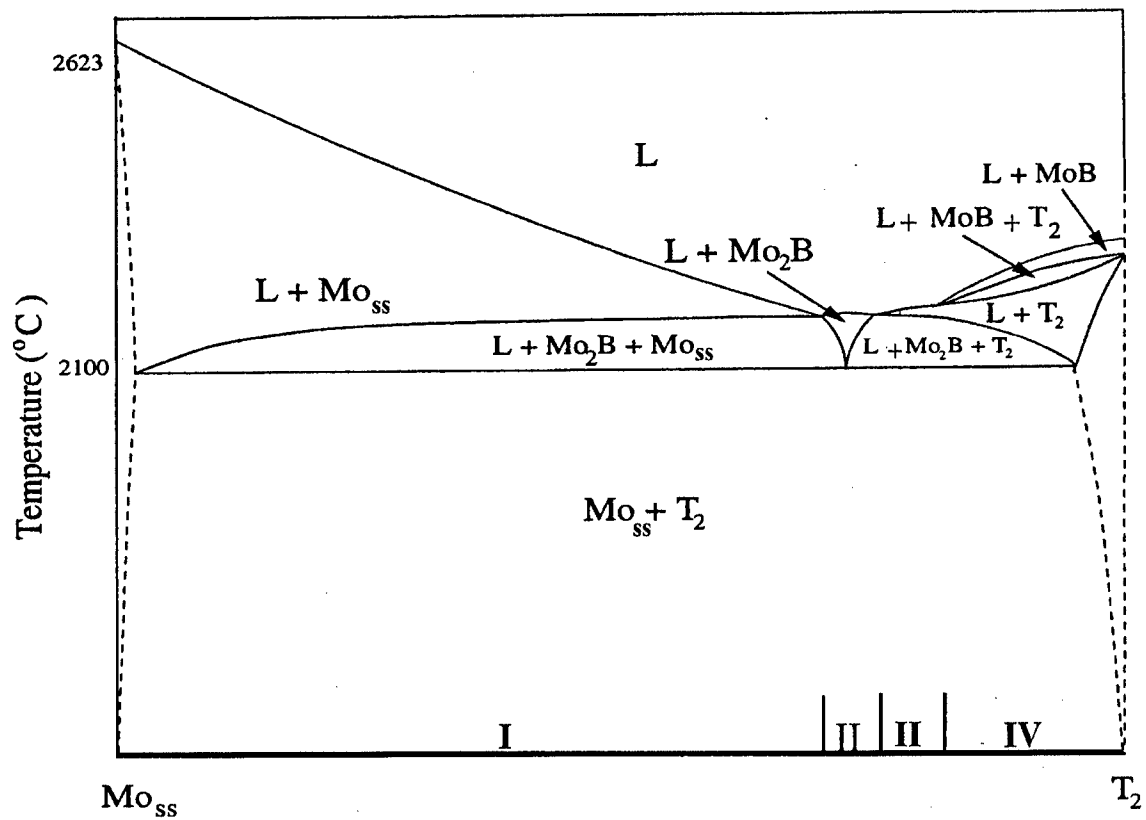


Figure 3 $\text{Mo(ss)} + \text{T}_2$ plethal section showing four types of primary solidification

3.5 Growth Kinetics Involving the T_2 Phase Formation

A diffusion study has been initiated to examine the formation of the T_2 phase between Mo_2B and Mo_5Si_3 . Figure 4 shows the back-scattered (BS) image of the cross section of the Mo_5Si_3/Mo_2B diffusion couple subject to 400 hrs annealing treatment at $1600^\circ C$. The EPMA analysis verified the Mo_2B phase on the far-left side, Mo_5Si_3 on the far-right side and the T_2 phase between Mo_2B and Mo_5Si_3 . In other words, one single phase T_2 appears in the Mo_2B/Mo_5Si_3 diffusion couple annealed at $1600^\circ C$ for 400 hrs. However, two phases – T_2 and Mo_3Si – were found in the Mo_2B/Mo_5Si_3 diffusion couples annealed at $1600^\circ C$ for 100 and 200 hours respectively. The T_2 phase initiated and grew from the Mo_2B phase, and the Mo_3Si phase initiated and grew from the Mo_5Si_3 phase.

In Figure 4 the T_2 phase exhibits flat interface with the Mo_2B phase, though its grain has columnar structure. The T_2 phase, however, does not have flat interface with the Mo_5Si_3 phase. In addition, the columnar grains closer to the Mo_5Si_3 phase are bigger than those to the Mo_2B phase. Moreover, cracks in the Mo_5Si_3 phase are stopped or diverted at the interface between Mo_3Si and Mo_5Si_3 (100 and 200 hrs annealed diffusion couple), and T_2 and Mo_5Si_3 (400 hrs annealed diffusion couple). This indicates that the T_2 and Mo_3Si phases have a toughness level sufficient to reduce crack propagation.

The Mo_3Si phase initiates and grows from the Mo_5Si_3 side in 100 and 200 hrs annealed diffusion couples, but is not uniformly produced along the Mo_5Si_3 phase. On the contrary, the Mo_3Si phase was not found in a diffusion couple annealed for 400 hours. The T_2 phase initiates and grows from the Mo_2B phase side due to Si atomic flow, but the T_2 layer thickness is only about $25\text{ }\mu m$ after 400 hrs annealing at $1600^\circ C$. However, disappearance of the Mo_3Si phase in the 400 hrs annealed diffusion couple indicates that in the Mo_3Si phase B atoms may diffuse faster than Si atoms. A key consequence of the changing phase sequence with annealing time is that the initial diffusion path is not in steady state, but reflects transient conditions. This behavior indicates another limitation of our current annealing capability. Annealing at $1600^\circ C$ for longer than 400hrs. is not reliable in our current system due to breakdown in thermocouples and deterioration in furnace atmosphere control.

The overall growth kinetics for the T_2 phase is presented in Figure 4 and demonstrates diffusion control. The solid line in Figure 4 was obtained using the interdiffusion coefficients of the T_2 phase and the theoretical solution for the solute concentration derived by Fujita *et al* [56Fuj]. The estimated growth rate constant for the T_2 phase is $9 \times 10^{-16}\text{ m}^2/\text{sec}$ at $1600^\circ C$. According to Bartlett *et al* [64Bar], the growth rate constant of the Mo_3Si phase is approximately $3.75 \times 10^{-14}\text{ m}^2/\text{sec}$ at $1600^\circ C$. The growth rate of the T_2 phase is about two orders of magnitude lower than that of the Mo_3Si phase. Moreover, as indicated in Figure 4 the growth behavior of the T_2 phase layer is influenced by the neighboring phases that change with time during annealing as the diffusion path approaches steady state. Thus, the extrapolation of short time growth behavior to long times is questionable. This effect is also likely to impact the analysis and interpretation of oxidation behavior. Clearly, diffusion anneals at temperatures above $1600^\circ C$ are required to insure steady state conditions that are needed for the evaluation of reliable diffusivity values.

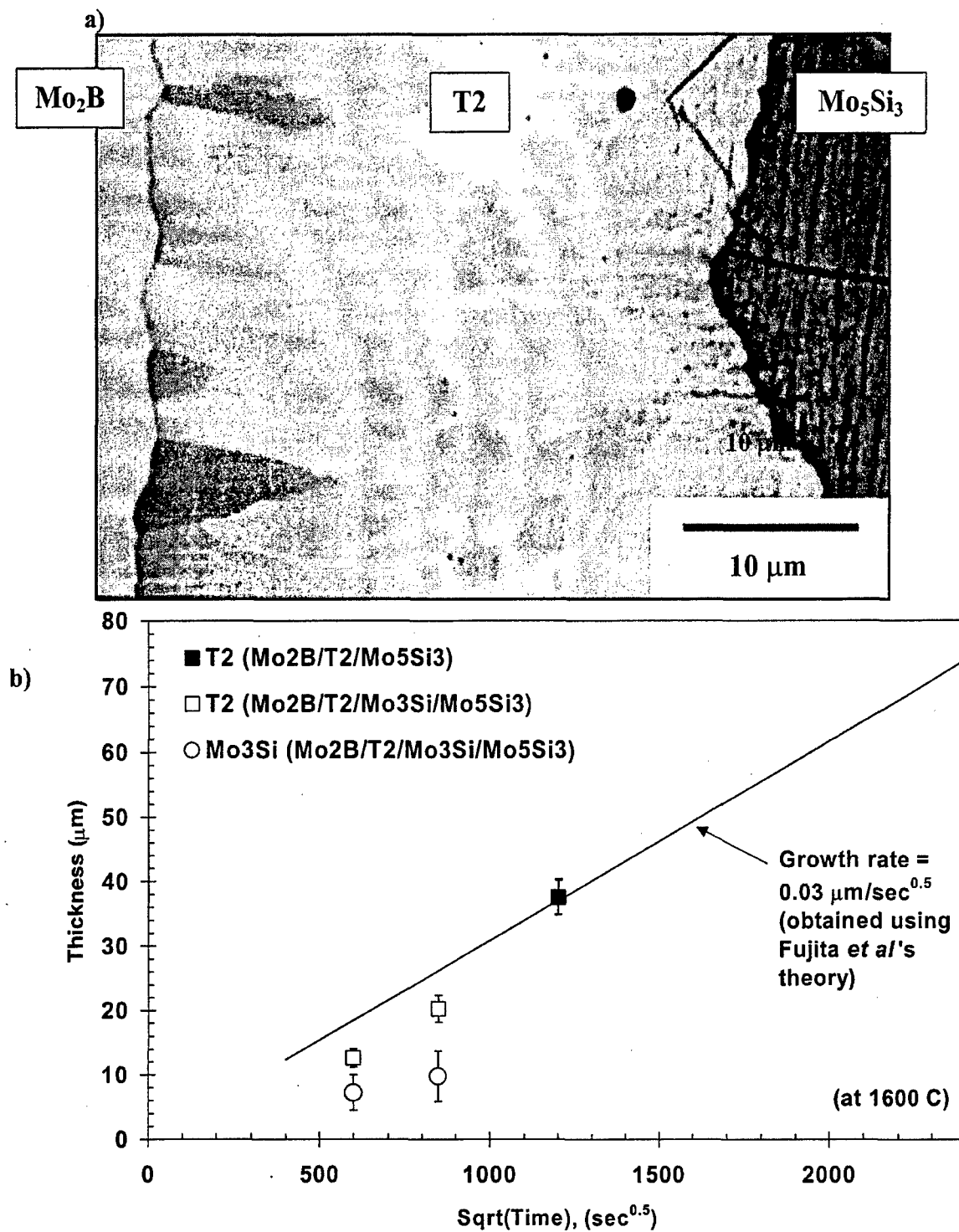


Figure 4 a) BSE images of the cross-section of diffusion couples annealed at 1600°C for 400 hours, b) concentration profiles of Si and B curve-fitted using the polynomial equations

3.6 Refractory Metal Substitution for Mo in the Mo-Rich Mo-B-Si Alloys

As indicated in the previous section on the solidification processing of the ac-cast alloys, the solidification segregation prevents the direct formation of either T_2 phase or the two-phase mixture directly from the melt. RSP has been shown to reduce the extent of segregation by essentially taking advantage of what appears to be a shallow liquidus surface on most of the Mo portion and thus a small degree of undercooling may only be needed to suppress the boride phase formation. Another approach that is being pursued is the substitution of some of the Mo atoms by some refractory metals such as Nb or Cr. The current results clearly indicate that if the stability of the two-phase field can be retained into the quaternary system by essentially expanding the phase field of both phases, the segregation can be reduced tremendously. For example, by substitution Nb for Mo, the two-phase field is continuously enlarged since Nb forms solid solution with Mo in bcc and T_2 phases. In fact, the compositions of the T_2 phase can be further extended to off-stoichiometric region primarily in the Si-rich area. The presence of nearby Nb_5Si_3 (T_2 phase) as a low temperature form in the Nb-Si binary section raises the possibility of a continuous solid solution of the T_2 phases at higher temperatures ($> 1600^\circ\text{C}$). Furthermore, if the solid solution does exist, it also confirms the strong stabilization effect of Boron of the T_2 structure. For reference, at a relatively low temperature (above 1650°C), the T_2 phase in Nb-Si system transforms into the T_1 phase. This consideration is clearly important in lieu of the fact that some of the important alloying design will involve the usage of refractory metal substitutions. It is therefore important to examine the role of B in the enhancing the phase stability of the T_2 structure. High temperature DTA will enable us to elucidate the effect of B in altering the phase transformation temperatures and to establish the complete phase relations of the two-phase field with the surrounding phases in the solid state. It should be noted here that based on the two-phase microstructure in Nb-substituted alloys subjected to a typical annealing treatment of 1600°C for 150 hours, very little evidence of enhanced coarsening effect can be noticed which may imply that the retention of the thermal stability of the T_2 phase. This may be supported by the fact that for very little depression in liquidus surface was found in extensively Nb-substituted Mo_5Si_3 , another metal-rich silicides. Nevertheless, quantitative assessment on the liquidus temperatures with respect to the effect of refractory metal substitution is very crucial in designing an effective alloying strategy.

3.7 New Research Opportunities

1. Coating strategy for thermal and diffusion barriers

A key performance capability for elevated temperature materials is environmental resistance. Under oxidizing conditions the development of an adherent oxide scale is the foundation of the environmental resistance. For Ni-base superalloys the protective oxide scale is based upon an Al_2O_3 surface layer which also exhibits a small parabolic rate constant, K_s . However, K_s is temperature dependent and at temperatures above about 1300°C the K_s for an SiO_2 layer is smaller than that for Al_2O_3 . Indeed this transition in surface oxide growth behavior is part of the design advantage provided by RM-Si-B systems. The steps in the oxidation of Mo-Si-B alloys lead to the development of a protective SiO_2 scale. Initially, MoO_3 forms

preferentially, but this layer offers no protection to continued oxidation. The MoO_3 layer is transient because it sublimates readily at temperatures above 900°C to leave a surface that is enriched in Si and B. The enriched surface then develops an SiO_2 layer that also contains B_2O_3 . The $\text{SiO}_2 + \text{B}_2\text{O}_3$ surface does restrict oxygen transport and provides a reduced oxygen activity so that MoO_2 forms at the base alloy surface. The cross sectional appearance of the base alloy surface scale following oxidation is shown in Figure 6a. While this layer is partially protective, it does not completely block O_2 transport so that with continued oxidation exposure, the thickness of the oxide increases along with a recession of the alloy base. In order to minimize the alloy recession two strategies are under active study. First, modifications to the $\text{SiO}_2 + \text{B}_2\text{O}_3$ scale are being examined to reduce O_2 mobility. One simple but effective way to do this is shown in Figure 6b where an additional thickness of SiO_2 is deposited on the $\text{SiO}_2 + \text{B}_2\text{O}_3$ surface layer. This treatment reduced the underlying MoO_2 layer thickness by a factor of two. Other additives are under study, but these additions will also include chemical with either the surface layer or the base alloy or both. At present we do not have a capability to monitor these reactions in a quantitative manner, but the requested DTA/TGA system will allow for a quantitative assessment and the determination of the reaction kinetics. The second approach to controlling oxidation is to use a thermal barrier coating which permits the base alloy temperature to be much lower than the actual service temperature (by about $200\text{--}300^\circ\text{C}$). The lower operating temperature will then naturally yield a much reduced base alloy recession. Thermal barrier coating (TBC) systems are currently under active development, but typically involve outer layers of low thermal conductivity oxides such as ZrO_2 which are applied with a controlled porosity to accommodate thermal expansion mismatch due to the thermal gradient. There are also additional layers in a TBC materials system for adhesion (bond coat) and diffusion barrier functions. Therefore a TBC is a complex materials system with several interface reactions of importance. Clearly, the qualitative observations that are possible with our current capability do not allow for a full evaluation of TBC stability. The necessary quantitative measurements and kinetics analysis can be provided by the requested DTA/TGA system.

2. Thermodynamic Evaluation

The current work on the determination of the isothermal sections at 1200 and 1600°C in the Mo-Si-B system is essentially completed. The important lesson from this experience concerning the requirement for long term annealing must be considered in all future work. Information on the temperature dependence of the solubility will be used to refine the plethral section that has been estimated between Mo(ss) and the T_2 phase. The temperature dependence of the lattice parameters gives the expansion coefficients for both the a - and c -axis parameters, which in turn provides a measure of the anisotropy in expansion behavior for the T_2 phase.

Another important issue in phase stability is the further analysis of existing information and the determination of other key data to allow for the development of a thermodynamic model for the T_2 phase. Towards this objective, further information on the constitutional defect mechanism that operates in the T_2 phase is necessary. The data required to establish the defect mechanism will be determined by careful measurement and analysis of lattice parameter versus composition trends, and x-ray peak intensity analysis for specific reflections provides an insight into site occupancy determination [83Spe,88Pen,96Ros]. The identification of the operative defect mechanism together with the phase equilibria measurements will provide the basis for the formulation of a thermodynamic model for the T_2 phase. Unfortunately, reliable thermodynamic data for the T_2 phase are not available. However, use of the thermodynamic data on phases that

coexist in equilibrium with the T_2 phase establishes reasonable bounds on the free energy of formation of the T_2 phase. At the present stage there are also clear limitations on the calculation method since it treats phases as line compounds. Nonetheless, this approach does illustrate the potential for a full analysis once measurements become available.

Using the thermodynamic data of boride and silicide phases and the following thermodynamic relations

$$S_T = S_{298} + \int_{298}^T \frac{C_p}{T} dT$$

$$\Delta H_T = \Delta H_{298} + \int_{298}^T C_p dT$$

the free energy of formation of each phase at 1600°C is evaluated (Table 1). The free energy of formation of Mo_2B_5 is estimated from the free energy diagram of the Mo-B binary system. In order for Mo_2B , MoB and Mo_2B_5 to exist as a stable phase at 1600°C, the rational value of the free energy of formation of Mo_2B_5 should be in between -93.09 and -130.55 kJ/g-atom. The mean value, -111.82 kJ/g-atom, is selected as the free energy of formation of Mo_2B_5 at 1600°C. On the basis of the phase stability shown in Figure 1, the free energy of formation of the T_2 phase is estimated as -130.9 ± 0.6 kJ/g-atom (or -1047.30 ± 5.29 kJ/mole). A linear regression on the free energies of formation of the T_2 phase at other temperatures yields $\Delta G_f = -100.34 - 0.505T$ (kJ/mole) for the T_2 phase

Table 1 The Estimated Free Energy of Formation at 1600°C

Phase	ΔG_f (KJ/mol)	Δg_f (KJ/g-mol)
B	-48.23	-48.23
Mo	-103.03	-103.03
Mo_2B	-371.33	-123.78
MoB	-253.48	-126.74
Mo_3Si	-504.15	-126.04
Mo_5Si_3	-1076.35	-134.54
$MoSi_2$	-390.44	-130.15
Si	-85.18	-85.18

Table 2 The Estimated Free Energy of Formation of T_2

Temperature		Free Energy of Formation (KJ/mole)
(°C)	(K)	
1200	1473	-845.39 ± 6.72
1300	1573	-893.70 ± 6.42
1400	1673	-943.50 ± 6.08
1500	1773	-994.72 ± 5.70
1600	1873	-1047.30 ± 5.29

The free energy planes of phases in the Mo-rich Mo-B-Si system including the T_2 phase can be established in terms of the widely used sublattice model, which treats a solution phase as the ordered arrangement of sublattices in the disordered conditions. The sublattice model approximates the enthalpy of mixing in terms of the nearest neighbor bond energies and the entropy of mixing in terms of random distribution of atoms within the sublattice [70Hil,45Tem,81Sun]. Ansara *et al.* [97Ans] and Huang [98Hua] shows that the sublattice model is very adequate to describe the thermodynamic properties of the ordered phases in the Ni-Al system that is characterized by five intermetallic compounds with different structures. In order to exam the sublattice model appropriate for the T_2 phase, the phase diagram data such as solidus, liquidus, or phase boundary composition and temperatures are necessary. Therefore, formulation of a thermodynamic model of the T_2 phase requires information of the defect structure, thermodynamic data and the phase diagram data.

- In order to identify the temperature dependence of the a - and c - lattice parameters at higher temperatures ($>1600^\circ\text{C}$), the single T_2 phase will be long-term annealed. X-ray diffraction analysis will determine those lattice parameters of the T_2 phase at very high temperatures. Determination of the a - and c -axis lattice parameters of the T_2 phases with different compositions provides information as to the defect structure, which explains broad compositional homogeneity region of the T_2 phase, and temperature dependence of lattice parameters.
- The high-temperature DTA also allows for measuring the heats of formation of the T_2 phases with different T_2 compositions by heating up powder mixture of binary boride and silicide alloys. The solidus and liquidus temperature data at different T_2 compositions, data of the heat of formation of the T_2 phase, and defect structure information will allow for formulation of a thermodynamic model for the T_2 phase, which provides phase equilibria at temperatures.
- Conventional solidification processing has been mitigated the problems associated with as-cast segregation. Rapid solidification has completely demonstrated that the segregation-induced formation of boride phases can be suppressed so that the single T_2 phase can be formed directly from the melt. However, the T_2 phase formed from the melt by rapid solidification processing is limited in size. This requires other processing technique to synthesize the composition-controlled, homogeneous and bulk T_2 phase. A single T_2 phase can be produced by blending the Mo_2B and Mo_5Si_3 powders and sintering it at very high temperatures ($> 1600^\circ\text{C}$), because diffusion couples between binary boride and silicide phases have been successfully constructed to allow for the synthesis of the T_2 phase during interdiffusion. In addition, annealing the powder mixture at higher temperature reduces the annealing time.

3. 8 RESEARCH RELATED EDUCATION

The design of materials for ultrahigh temperature service is one of the most demanding challenges confronting contemporary materials science efforts. These materials are truly enabling components that are rate limiting in a number of key technologies involved in energy production, transportation and aerospace propulsion systems. Our research in this area has

captivated the interest and attention of numerous students. In both the undergraduate and graduate courses offered by the PI, real examples of ultrahigh temperature materials behavior are used to intrigue and interest students. Outside of the classroom the PI employs four to six undergraduates within his research group. The undergraduate students are active participants along with the graduate students in our ONR and AFOSR projects. Several of our former graduate students are currently employed in industry or National Laboratories where they continue to work on high temperature structural materials. From this background of educational experience in high temperature materials at the University of Wisconsin-Madison the intention is to continue and to expand the activities with the facilities requested in the proposal. For example, the high temperature annealing furnace will allow for the development of student projects dealing with interdiffusion behavior and coating development. Currently, the temperature limitation of the existing facility requires such extended annealing times that it does not allow for the scheduling of any extra work necessary to accommodate undergraduate project studies. Similarly, our current low temperature DTA facility ($T < 1500^{\circ}\text{C}$) limits the ability to incorporate student projects. The requested DTA/TGA system will not only enable a new scope of high temperature phase stability studies, but also will allow for the first time new studies based upon the analysis of reaction kinetics. It should be added that the facilities will be brought online by the graduate students. We have had a remarkable and a very satisfactory experience with undergraduate use of the facilities. It turns out that many undergraduates are highly motivated by the opportunity to use state-of-the-art equipment and this motivation further motivates the graduate students in a synergistic way.

References

- [98Hua] HUANG, W. and CHANG, Y.A., *Intermetallics*, 6, 487, 1998
- [97Ans] ANSARA, I., DUPIN, N., LUKAS, H.L. and SUNDMAN, B., *J. Alloys and Comp.*, 247, 20, 1997
- [97Nun] NUNES, C.A., SAKIDJA, R. and PEREPEZKO, J.H., in *Structural Intermetallics 1997* (edited by Nathal, M.V., Darolia, R., Liu, C.T., Martin, P.L., Miracle, D.B., Wagner, R. and Yamaguchi, M.), 831, 1997
- [96Ros] ROSSOUW, C. J., FORWOOD, C. T., GIBSON, M. A. and MILLER, P. R., *Phil. Mag. A*, 74, 57, 1996 & 74, 77, 1996
- [92Asm] ASM HANDBOOK Vol 3 ALLOY PHASE DIAGRAMS, ASM International, Ohio, USA, 1992
- [88Pen] PENNYCOOK, S.J., *Ultramicroscopy*, 26, 239, 1988
- [87JCP] JCPDS. Powder Diffraction File. International Centre for Diffraction Data. Swarthmore, PA. Card # 9-292, 1987
- [83Smi] *Smithells Metals Reference Book* 6th edition (ed. Brandes, E. A.), Butterworths, 13-11, 1983
- [83Spe] SPENCE, J.C.H. and TAFT, J., *J. Microscopy*, 130, 147, 1983
- [81Sun] SUNDAMAN, B. and AGREN, J., *J. Phys. Chem. Solids*, 42, 297, 1981
- [70Hil] HILLERT, M and STAFFANSON, L.-I., *Acta Chem. Scand.*, 24, 3618, 1970 [68Sne] SNETSINGER, K.G., BUNCH, T.E and KEIL, K., *American Mineralogist*, 53: 1770, 1968
- [64Bar] R. W. BARTLETT, P. R. GAGE AND P. A. LARSEN, *Trans AIME*, 230: 1528, 1964.
- [60Aro] ARONSSON, B. *Acta Chem. Scand.* 14 : 1414, 1960

[56Fuj] H. FUJITA AND L. J. Gosting, J. Am. Chem. Soc., 78, p1099, 1956
[45Tem] TEMKIN, M., Acta Phys. Chim., 20, 411, 1945

UNCLASSIFIED

[This page is intentionally left blank.]

UNCLASSIFIED